

# Comparative Analysis of some Low-Complexity Blind Synchronization Algorithms for IR-UWB Systems

Rizwan Akbar, Emanuel Radoi, Stéphane Azou

Université Européenne de Bretagne, Université de Brest; CNRS, UMR 6285 Lab-STICC

6 avenue Victor Le Gorgeu, CS 93837, 29238 Brest cedex 3, France

Email: {Rizwan.Akbar, Emanuel.Radoi, Stephane.Azou}@univ-brest.fr

**Abstract**—Ultra wideband (UWB) radio has emerged as an attractive candidate for short-range wireless communications in recent years due to its unique features. However, implementation of UWB radios in order to utilize these features is coupled with some pronounced design challenges. To achieve precise timing synchronization is one of the most crucial task among them and is a key factor to ensure a reliable performance of such systems. In this paper, we present an overview and comparative study of three synchronization algorithms which provide efficient performance under unique signal and channel characteristics of UWB. These algorithms employ cross-correlation, PN code matching and energy detection operations respectively to achieve synchronization. The performance is then analyzed by numerical results under realistic propagation environment that takes into account the severe multipath and inter-frame interference (IFI). Also, hardware complexity and acquisition speeds of these algorithms are discussed.

**Index Terms**—Impulse radio ultra wideband (IR-UWB), time hopping (TH), synchronization, dirty template, asymmetric modulation, code matching

## I. INTRODUCTION

Ultra wideband (UWB) radio has been drawing plentiful attention among researchers since its approval as commercial technology for data communications as well as for radar applications by Federal Communication Commission (FCC) in February 2002 [1]. A large swathe of 7.5 GHz spectrum in 3.1-10.6 GHz range with extremely low power spectral density of -41.25 dBm/MHz is allocated for UWB communications, thus the name ultra wideband. Impulse radio UWB (IR-UWB) [2] and multiband OFDM based UWB [3] have emerged as the two potential candidates for implementing UWB systems. Addressing synchronization issue in IR-UWB systems, which are characterized by data transmission using trains of nanosecond level pulses, is the focus of this paper. The interest in IR-UWB is attributed to many unique features such as its ability to coexist with licensed narrowband systems in underlay mode, simple baseband transceiver, low probability of interception and detection, high ranging resolution and ability to exploit rich multipath diversity [4].

The aforementioned attractive features, however, come at a cost of equally demanding design challenges such as dense multipath channel estimation, precise synchronization, operation under severe interference from overlay systems, supporting multiple-access and receiver design. The stringent timing requirements pose a major challenge to the deployment of IR-UWB and timing accuracy is fundamental to ensure a satisfactory performance of such systems. The synchronization is typically performed in two stages in IR-UWB systems. During the first stage, called acquisition stage, a coarse synchronization is carried out to quickly identify the symbol starting frame. The second stage, known as the tracking stage, aims at refining the acquisition stage estimator and boiling down the timing mismatch to less than a chip duration.

Different type of receivers need different levels of synchronization accuracy. The optimal coherent receiver (Rake) needs to align a locally generated template with the incoming received signal with an accuracy at the order of signal bandwidth reciprocal, which for UWB is in the order of tens of picoseconds. The low complexity noncoherent receivers (Transmitted Reference, Differential Detector, etc.) slightly relax the synchronization requirements and typically need an accuracy at the order of tens of nanoseconds [5]. Nevertheless, in both cases the synchronization requirements remain very strict. It was shown in [6]–[8] that a slight misalignment at the order of nanoseconds can severely degrade the IR-UWB systems performance.

Thus, the need of nanosecond-level precision using low power UWB pulses makes synchronization in UWB much more tough task to accomplish than in other communication systems. Furthermore, the fine resolution obtained thanks to the wide signal bandwidth results in large search space for the synchronizer while extremely low power transmission means long sequence to be processed in order to develop a reliable synchronization criterion. Many resolvable multipaths due to short UWB pulses can also cause the receiver to lock with more than one arriving multipath component, thus resulting in multiple acquisition phases. And last but not least, the transmitted signal is distorted by antennas and unknown frequency selective dense multipath channels [9], [10], which further intricate the already challenging task.

Manuscript received October 20, 2011; revised February 22, 2012; accepted March 25, 2012.

This work was supported in part by Higher Education Commission (HEC), Pakistan.

Due to these reasons, synchronization has been much emphasized by UWB researchers and several timing algorithms have been proposed in past. In this paper, we will provide a literature survey and then will limit our comparative study to three blind synchronization algorithms which are selected for the interesting trade-off they provide between performance and complexity level. The rest of this paper is organised as follows. Section II describes signal format and preliminaries. In section III, overview of synchronization algorithms is given. Comparative study about computational complexity of studied algorithms is presented in sections IV. Finally, simulations results are provided in section V to corroborate the discussion while conclusions are summarized in section VI.

## II. SYSTEM MODEL AND PRELIMINARIES

It is important to understand first the propagation channel and transmission model for UWB systems in order to better understand the synchronization problematic. The transmitted signal in IR-UWB radio for point-to-point link equipped with symbol periodic time-hopping (TH) codes can be expressed as

$$s(t) = \sum_n a_n p_T(t - nT_s) \quad (1)$$

where  $p_T(t) = \sum_{j=0}^{N_f-1} p(t - jT_f - c_jT_c)$  is symbol-long waveform of duration  $T_s = N_fT_f$  consisting of  $N_f$  frames each of duration  $T_f$  and  $\{a_n\}$ 's are information-bearing symbols taking values  $\pm 1$  with equal probability. An ultra-short UWB waveform  $p(t)$  of duration  $T_p \ll T_f$  is transmitted one per frame which means that  $N_f$  waveforms are used to represent one data symbol. This is one principle contradiction of IR-UWB systems compared to narrowband systems where one waveform represents multiple binary elements. These UWB pulses are time shifted by integer multiples of chip duration  $T_c = \lfloor T_f/N_c \rfloor$  in each frame by a pseudo-random TH code  $\{c_j\}_{j=0}^{N_f-1} \in [0, N_h - 1]$  with  $N_h \leq N_c$ , where  $N_c$  is the number of chips per frame satisfying  $T_f = N_cT_c$ . These TH codes serve dual purpose of spectral smoothing along with enabling multiple access by adopting user-specific codes.

The UWB channel can be modeled as a tapped-delay line [10], [11] whose impulse response can be denoted as  $h(t) = \sum_{l=0}^{L-1} \lambda_l \delta(t - \tau_l)$ , where  $\{\lambda_l, \tau_l\}_{l=0}^{L-1}$  are channel path gains and delays respectively, satisfying  $\tau_l < \tau_{l+1}, \forall l$ . These channel coefficients are assumed invariant over one transmission burst due to quasi-static nature of UWB channel, but are allowed to vary across bursts. Typically, UWB channel's rms delay spread ( $\tau_{rms}$ ) satisfies:  $\tau_{rms} \gg T_p$ , thus inducing ISI, and channel's coherence time ( $T_{coh}$ ) satisfies:  $T_{coh} \gg T_p$ , resulting in slow fading. Letting the relative path delay as  $\tau_{l,0} := \tau_l - \tau_0$ , the signal at the receiving end is the convolution  $s(t) \star h(t - \tau_0)$  in the presence of AWGN noise  $w(t)$  with double-sided power spectral density  $N_0/2$ , given by

$$r(t) = \sum_n a_n p_R(t - nT_s - \tau_0) + w(t) \quad (2)$$

where  $p_R(t) = \sum_{j=0}^{N_f-1} g(t - jT_f - c_jT_c)$  is the aggregate received symbol waveform of duration  $T_R$ , with  $g(t) = \sum_{l=0}^{L-1} \lambda_l p(t - \tau_{l,0})$  representing single UWB dispersed pulse of duration  $T_g$ . Evidently, by selecting  $(N_h - 1)T_c + T_p + \tau_{L,0} \leq T_f$ , we can avoid both IFI and ISI, while choosing  $T_p + \tau_{L,0} \leq T_f$  and  $c_{N_f-1} = 0$  will ensure again no ISI but will allow IFI. Our objective is to estimate the timing offset  $\tau_0$  in the absence of any knowledge about transmitted sequence and multipath channel.

## III. SYNCHRONIZATION ALGORITHMS

A number of algorithms treat synchronization as a part of channel estimation and aim at joint estimation of timing and channel taps [12]–[14]. In [12], this is done using maximum-likelihood (ML) criterion and is applicable in both data-aided (DA) and non data-aided (NDA) context. A formidably high sampling rate up to several GHz along with suboptimal estimation in case of closely spaced multipaths raise concerns over its implementation. A least squared based method is presented in [13] which look for the minimum of Euclidean distance between received signal samples and a local replica of their noiseless components. However, it involves two dimensional searching along with very high sampling rate, making it computationally complex. Besides, it may require very fast analog-to-digital converters (ADC) as it is a fully digital approach. Another joint channel estimation and synchronization scheme developed in [14] employs subspace method. The timing estimation is converted to a harmonic retrieval problem and is solved using subspace analysis. The implementation complexity involved in subspace analysis along with possible ill-conditioned Vandermonde systems in closely spaced multipaths limits its application to realistic UWB scenarios. Several other algorithms based on low complexity ML [15], cyclostationarity [16] and first-order statistics [17] have also been studied. However, most of these algorithms require certain assumptions such as absence of time-hopping (TH) codes, absence or known multipath, no inter-frame interference/inter-symbol interference (IFI/ISI) etc, which are rather optimistic for practical UWB settings.

The design of low-complexity synchronization schemes using either symbol-rate or frame-rate sampling is therefore highly motivated in UWB in order to reduce the implementation complexity. Peak-picking the cross correlation samples of the received signal and a locally generated template is the traditional approach to establish synchronization. However, the template must include the channel effect which is difficult as the channel impulse response is usually unknown during the synchronization stage. A scheme, called Timing with Dirty Templates (TDT) [18] and its variants [19], [20] have been proposed to solve this problem using symbol-rate sampling. Relying on periodic transmission of non-zero mean symbols, a group of joint timing and template recovery algorithms have been developed in [21]–[25], with universal applicability in the presence of ISI and multiuser interference (MUI). Capitalizing on the fine correlation properties

of binary codes, various algorithms have been proposed in [26]–[28], which provide much improved performance using fewer number of symbols.

In the sequel, we will focus and explain in detail three algorithms that are correlation based timing with dirty templates proposed in [18], orthogonal code matching based method in [26] and energy detection based method presented in [22]. The reasons of choosing these methods are: 1) they are simple as they need either symbol-rate or frame-rate sampling, 2) both DA and NDA variants are possible, 3) they are functional under practical UWB operating settings and 4) they can provide synchronization up to any desired resolution.

**A. Timing with Dirty Template (TDT)**

The simplest approach for synchronization in impulse radio is based on match-filtering the received signal with a locally generated "clean template" and peak-picking the correlation samples. Evidently, the reference template must encompass multipath channel effect which is unknown at synchronization, thus needing a cumbersome task of channel estimation. A scheme, known as timing with dirty templates (TDT), was proposed in [18] to tackle this issue by utilizing pair of successive symbol long segments of  $r(t)$ , where one segment serves as template for the other. These segments are termed as "dirty templates" because they are i) noisy, ii) distorted by unknown channel and iii) subject to unknown timing offset  $\tau_0$ . Knowledge about multipath channel and TH codes becomes unnecessary as this information is embedded in dirty templates and thus improves energy capture.

The basic idea behind TDT hinges upon finding the maximum of square of symbol-rate samples, obtained by simple integrate-and-dump operation performed on the products of dirty templates. Both NDA and DA variants of TDT are proposed in [18] where the former are bandwidth efficient while the latter enjoy fast synchronization. In the absence of MUI and ISI, the timing offset  $\tau_0$  can be estimated in NDA-TDT as

$$\hat{\tau}_0 = \arg \max_{\tau \in [0, T_s]} J_{nda}(\tau)$$

$$J_{nda}(\tau) = \frac{1}{K} \sum_{k=1}^K \left( \int_{2kT_s}^{(2k+1)T_s} r(t + \tau)r(t + \tau - T_s)dt \right)^2 \tag{3}$$

where  $K$  is the number of symbol-long pairs. To grasp the gist of TDT, first the symbol-rate samples are obtained by integrate-and-dump operation as

$$x_k(\tau) = \int_0^{T_s} r(t + 2kT_s + \tau)r(t + (2k - 1)T_s + \tau)dt \quad \forall k \in [1, +\infty), \tau \in [0, T_s) \tag{4}$$

Ignoring the noise brevity, the received waveform can be represented using (2) as

$$r(t + kT_s + \tau) = \sum_n a(n)p_R(t - T_s + \tau_0 + kT_s + \tau) \tag{5}$$

Assuming that the non-finite support  $T_R$  of  $p_R(t)$  is upper bounded by symbol duration  $T_s$  to avoid ISI, it is obvious that only two adjacent values of  $n$  will contribute nonzero summands in (5). Thus (5) is simplified as

$$r(t + kT_s + \tau) = a(k - 1)p_R(t + T_s - \tilde{\tau}_0) + a(k)p_R(t - \tilde{\tau}_0) \tag{6}$$

$\forall t, \tau \in [0, T_s)$ , where  $\tilde{\tau}_0 := [\tau_0 - \tau]_{\text{mod } T_s}$ . Substituting (6) in (4), we get

$$x_k(\tau) = a(2k - 1)[a(2k - 2)\varepsilon_A(\tilde{\tau}_0) + a(2k)\varepsilon_B(\tilde{\tau}_0)] \tag{7}$$

where  $\varepsilon_A(\tilde{\tau}_0) = \int_{T_s - \tilde{\tau}_0}^{T_s} p_R^2(t)dt$  and  $\varepsilon_B(\tilde{\tau}_0) = \int_0^{T_s - \tilde{\tau}_0} p_R^2(t)dt$ . The mean square of samples in (7) can be written as

$$E\{x_k^2(\tau)\} = \varepsilon_A^2(\tilde{\tau}_0) + \varepsilon_B^2(\tilde{\tau}_0) = \frac{1}{2}[\varepsilon_A(\tilde{\tau}_0) + \varepsilon_B(\tilde{\tau}_0)]^2 + \frac{1}{2}[\varepsilon_A(\tilde{\tau}_0) - \varepsilon_B(\tilde{\tau}_0)]^2 \tag{8}$$

Now observe that  $\varepsilon_A(\tilde{\tau}_0) + \varepsilon_B(\tilde{\tau}_0) = \int_0^{T_s} p_R^2(t)dt = \varepsilon_R$  is the constant energy of the aggregate template and does not contain any information. However, the energy difference  $\varepsilon_B(\tilde{\tau}_0) - \varepsilon_A(\tilde{\tau}_0)$  is uniquely maximized at  $\tilde{\tau}_0 = 0$  or equivalently  $\tau = \tau_0$ , since  $\varepsilon_A(\tilde{\tau}_0)$  is minimized at  $\tilde{\tau}_0 = 0$  and  $\varepsilon_B(\tilde{\tau}_0)$  is maximized at  $\tilde{\tau}_0 = 0$ , by definition. Thus,  $E\{x_k^2(\tau)\}$  can be considered as a sufficient criterion for estimating  $\tau_0$ . Replacing ensemble mean with its sample mean estimator using  $K$  pairs of symbol long received segments will eventually return the objective function  $J_{nda}(\tau)$  of (3). A block diagram of NDA-TDT algorithm is given in Fig. 1.

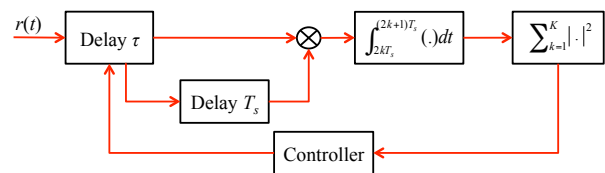


Figure 1. Block diagram of Non-data-aided Timing with Dirty Templates (NDA-TDT) Algorithm.

To speed up acquisition, a data-aided (DA) variant of NDA-TDT is possible using training sequence of  $a(n) = (-1)^{\lfloor \frac{n}{2} \rfloor}$ . This training pattern will reduce ensemble mean in (8) to  $E\{x_k^2(\tau)\} = [\varepsilon_A(\tilde{\tau}_0) - \varepsilon_B(\tilde{\tau}_0)]^2$  in noiseless case. Thus, in principle, as few as four symbols are sufficient for reliable estimation at high SNR. The performance in DA-TDT can be further improved by swapping the order of correlation and averaging in (3), thus developing a new criterion for estimating  $\tau_0$  as

$$\hat{\tau}_0 = \arg \max_{\tau \in [0, T_s]} J_{da}(\tau)$$

$$J_{da}(\tau) = \left( \int_0^{T_s} \tilde{r}(t + \tau)\tilde{r}(t + \tau - T_s)dt \right)^2 \tag{9}$$

where

$$\tilde{r}(t) = (-1)^{\lfloor t/2T_s \rfloor} \bar{r}(t) \bmod 2T_s$$

$$\bar{r}(t) = \frac{1}{K} \sum_{k=1}^k (-1)^k r(t + 2kT_s), \quad t \in [0, 2T_s]$$

This criterion provides best performance because using  $\tilde{r}(t)$  in cost function  $J_{da}(\tau)$  will reduce power spectral density of AWGN term to  $N_0/2K$ , thanks to averaging.

### B. Timing with Code Matching (TCM)

The methods in this class are based on exploiting the discriminative nature of well-designed polarity codes. The proposal in [26] relies on code matching and signal aggregation of one frame-long segments followed by averaging. The transmitted symbol is multiplied with a polarity code  $\{d_j\}_{j=0}^{N_f-1}$ , resulting in  $p_T(t) = \sum_{j=0}^{N_f-1} d_j p(t - jT_f - c_j T_c)$  and consequently  $p_R(t) = \sum_{j=0}^{N_f-1} d_j g(t - jT_f - c_j T_c)$ . The estimate of  $\tau_0$  is obtained by the optimization given as

$$\hat{\tau}_0 = \arg \max_{\tau \in [0, T_s]} J_{tcm}(\tau)$$

$$J_{tcm}(\tau) = \frac{1}{K} \sum_{k=1}^K \int_0^{T_I} \left| \sum_{j=0}^{N_f-1} d_j g_r(t) r(t + t_{k,j} + \tau) \right|^2 dt \quad (10)$$

where  $t_{k,j} = kT_s + jT_f + c_j T_c$ ,  $d_j g_r(t)$  is the correlation template for  $j^{th}$  frame and  $T_I$  is the integration interval. In words, the idea is simply to take frame long segments of same symbol, time shift them using TH codes and bi-polarize them by  $d_j$  at transmitter. At receiver, the synchronizer compensates for TH codes using *a-priori* knowledge and polarity change due to  $d_j$  followed by superimposition. Due to judiciously designed polarity code, this superimposition will result in constructive sum only if  $\tau = \tau_0$  and consequently  $J_{tcm}(\tau)$  will capture maximum energy given by  $J_{tcm}(\tau_0) = N_f^2 \int_0^{T_g} g^2(t) dt$ . Otherwise, if  $\tau \neq \tau_0$ , this superimposition will result in destructive addition, thus capturing much smaller energy. A block diagram of algorithm is provided in Fig. 2.

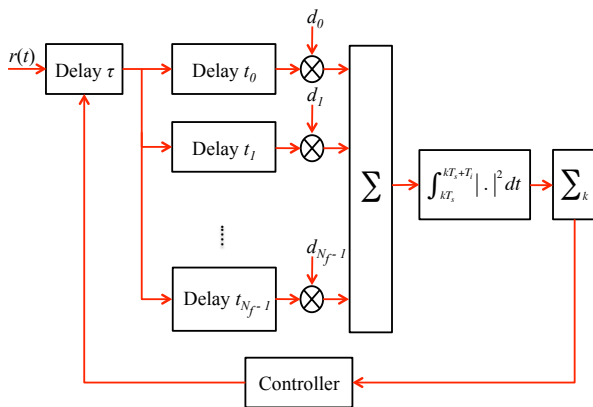


Figure 2. Block diagram of Timing with code matching (TCM) algorithm.

It is clear from (10) that the accuracy of estimation depends on both  $d_j g_r(t)$  and value of  $T_I$ , which determine the amount of energy captured in each integration. Ideally, maximum SNR is achieved at receiver by setting  $g_r(t) = g(t)$ , however this is practically infeasible as only partial information about channel is available during synchronization phase such as channel power delay profile (PDP) or maximum delay spread ( $\tau_{max}$ ). However, setting  $g_r(t) = 1$  can also ensure a reliable estimation while simplifying the implementation at the same time. This effectively reduces correlation template  $d_j g_r(t)$  to  $d_j$ , thus the suitable design of polarity codes is non-trivial for the algorithm to perform well. These codes must satisfy the two periodic autocorrelation functions (PACF) defined as

$$R_d^+[n] = \frac{1}{N_f} \sum_{j=0}^{N_f-1} d_j d_{(j+n) \bmod N_f}$$

$$R_d^-[n] = \frac{1}{N_f} \left( \sum_{j=0}^{N_f-n-1} d_j d_{j+n} - \sum_{j=N_f-n}^{N_f-1} d_j d_{(j+n) \bmod N_f} \right) \quad (11)$$

in such a way that their off-peak autocorrelation coefficients are as small as possible. There are many codes available which meet this constraint for the positive periodic ACF  $R_d^+[n]$  such as Barker codes, M-sequences etc. However, due to blind synchronization, the two consecutive BPSK symbols may be different, thus the code design must also take into account the negative periodic ACF  $R_d^-[n]$ . A minimax criterion to design these codes along with some optimal codes for certain values of  $N_f$  are listed in [26].

The other important parameter in (10) is the value of  $T_I$  can be set as  $T_g$  ideally, if information about maximum channel delay spread is known to receiver. Otherwise,  $T_I$  can be replaced by an upper bound on maximum dispersion or even by  $T_f - N_h T_c$ .

### C. Timing with Energy Detection (TED)

Low-complexity synchronization is possible via energy detection based methods which rely on exploiting the portion of received signal with significant energy, introduced specifically to enable synchronization. An interesting ISI and multi-user interference (MUI) resilient method was proposed in [22], which relies on intermittent transmission of nonzero mean symbols deliberately introduced by changing the modulation constellation at transmitter. During synchronization phase, one asymmetric BPSK symbol taking values  $(\theta, -1)$  equiprobably with nonzero mean:  $\mu = 0.5\theta + 0.5(-1)$ , with  $\theta > 1$ , is transmitted for every  $(M - 1)$  zero mean symbols where  $M = \lceil T_R/T_s \rceil + 1$  is channel delay spread dependent integer. Under the condition that AWGN and MUI are zero mean,

the timing offset  $\tau_0$  can be estimated by

$$\hat{\tau}_0 = \arg \max_{\tau \in [0, MT_s]} J_{ted}(\tau)$$

$$J_{ted}(\tau) = \int_0^{T_R} |\bar{r}((t + \tau) \bmod MT_s)|^2 dt \quad (12)$$

where  $\bar{r}(t) = \frac{1}{K} \sum_{k=0}^{K-1} r(t + kMT_s)$ ,  $t \in [0, MT_s]$  is the sample mean estimator of  $r(t)$  across  $K$  segments each of size  $MT_s$ . This mean of  $r(t)$  will comprise zero guards of size  $MT_s - T_R \geq T_s$ , which will be exploited by energy detector to estimate  $\tau_0$ . This in turn implies another condition for the algorithm to function properly which is that there should be no interval larger than  $T_s$  where  $p_R(t) = 0$  over its support  $[0, T_R]$ . This can be met by choosing symbol period  $T_s \geq \Delta\tau_{\max} - [(N_f - 1)T_f + c_{N_f-1}T_c + T_g]$ , where  $\Delta\tau_{\max} \geq \max_{l \in [1, L]} (\tau_l - \tau_{l-1})$  is the maximum successive channel delay difference. If this condition is not respected, then there will be multiple zero guards in  $\bar{r}(t)$  rendering the algorithm non-functional. The condition of zero mean MUI is satisfied if there is only one user responsible for synchronization in a network while others are transmitting zero mean interfering symbols, which is usually the case in ad-hoc networks. A block diagram of algorithm is given in Fig. 3.

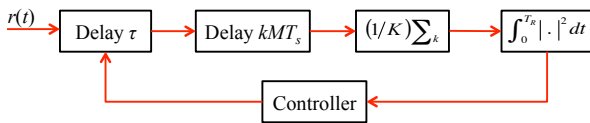


Figure 3. Block diagram of Timing with energy detection (TED) algorithm.

#### IV. COMPUTATIONAL COMPLEXITY ANALYSIS

Regarding implementation complexity, the methods described in previous section are particularly interesting as they can be computed either digitally or in analog form. All of these methods needs symbol-rate sampling, thus relaxing the subpulse rate sampling needed in [12], [13]. Analog delays to shift received signal segments by  $2T_s$  or  $t_{k,j}$  or  $MT_s$  are required in analog approaches which can be challenging. On the other hand digital domain implementation needs very high sampling rate in UWB regime. Nevertheless, one can adapt according to available resources, thus providing flexibility. As far maximization algorithms itself, each objective function needs a serial search which is not efficient and result in increased mean synchronization time. There are other search strategies possible, however their reduced mean synchronization time comes at a cost of lesser performance and rather strict conditions. Due to prohibitive complexity involved in linear search, usually the objective function is evaluated over a grid of equispaced  $N_\delta = \lfloor T_s/T_\delta \rfloor$  discrete bins each of duration  $T_\delta$  to estimate  $\hat{\tau}_0 = \hat{n}T_\delta$ . It is worth mentioning that synchronization is possible at any desired resolution and is only constrained by the affordable complexity.

As for the assumptions or a-priori knowledge are concerned, NDA-TDT is ideal as it needs no information whatsoever about transmitted signal. But its operation is quite limited and not applicable in ISI and MUI scenarios. DA-TDT shows resilience to MUI but not to ISI. A-priori information about user's TH codes and also about  $\tau_{max}$  are needed to select optimal value of  $T_I$  in TCM. It has been seen by simulations that when  $T_I > T_g$ , there is a plateau corresponding to same maximum in cost function  $J_{tcm}(\tau)$ , thus introducing ambiguity, while when  $T_I < T_g$  the maximum may drift from original  $\tau_0$ . So value of  $T_I$  has a considerable impact on synchronization accuracy in TCM. Same is true for TED which also needs information about  $\tau_{max}$  and at least about  $c_{N_f-1}$  to select  $T_R$ . It is worth stressing here that  $T_R$  is not only needed by synchronizer to select integration region but is also required by transmitter to select integer  $M$  which is used to decide about symmetric and asymmetric modulated symbols. Another disadvantage of TED is the aggravate SNR at receiver due to asymmetric modulation, which will deteriorate BER performance significantly during synchronization phase at least.

#### V. SIMULATIONS AND COMPARISONS

In this section, we will provide some preliminary simulation results to validate our discussion and will analyze how these methods behave in different operating conditions. A UWB pulse generated using B-spline based approach [29] is employed in simulations, which utilizes FCC mask efficiently. The channel model used is indoor multipath channel proposed by IEEE 802.15.3a working group [11]. Timing offset  $\tau_0$  is randomly generated from a uniform distribution over  $[0, T_s)$  at each Monte Carlo trial. We have focused only on frame-level coarse synchronization to keep the simulation time within acceptable limit i.e. we set  $T_\delta = T_f$ . Each symbol consists of  $N_f = 13$  frames. The remaining parameters are selected according to different operating conditions which are explained as follows :

**Test A. IFI/ISI Free:** To avoid any interference among frames and symbols, we select  $T_c = T_p = 1.28\text{ns}$ ,  $N_c = 20$  resulting in frame duration  $T_f = 25.60\text{ns}$  and  $N_h = 5$ . The channel used is the indoor multipath channel CM1, having rms delay spread  $\tau_{rms} = 5\text{ns}$  and truncated beyond  $T_f - N_h T_c$  to avoid IFI/ISI.

**Test B. IFI Present:** Next we consider the case which includes IFI but no ISI. This is achieved in simulations by selecting  $N_h = 10$  and  $c_{N_f-1} = 0$ . The channel now is truncated beyond  $T_f - T_c$ . In the worst case, these setting will cause  $9 * T_c$  long tail of multipath channel in the subsequent frame.

**Test C. ISI Present:** To allow ISI, we consider a much severe case by selecting CM4 channel of IEEE 802.15.3a standard, which has  $\tau_{rms} = 25\text{ns}$ . The channel is truncated beyond 50ns and energy normalized,  $T_f$  is reduced to 10ns and we avoid TH codes to observe the impact of ISI only. Clearly, by these setting each frame is affecting the subsequent 4 frames and each symbol is disturbing

the first 4 frames of next symbol.

**Test D. MUI Present:** We return to the original setting of Test A, but this time we assume that there are two interfering users also present in the system. We have assumed that the two users also employ the same polarity codes as the synchronizing user, but certainly different TH codes in case of TCM. For TED, they are supposed to transmit usual BPSK symbols.

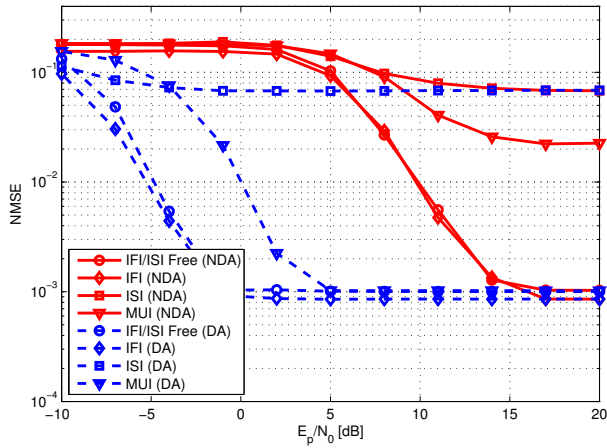


Figure 4. Performance of TDT synchronizer in both NDA and DA mode with  $K = 64$  pairs of dirty templates.

The NMSE (normalized mean square error w.r.t  $T_s^2$ ) performance of three methods under these scenarios is plotted as a function of  $E_p/N_0$  (where  $E_p$  is the energy of basic UWB pulse) in Figs. 4, 5 and 6. The floor in each figure is due to coarse synchronization employed will alleviate with increased resolution. One can observe the significant improvement in performance using DA version of TDT in Fig. 4. The performance under Test

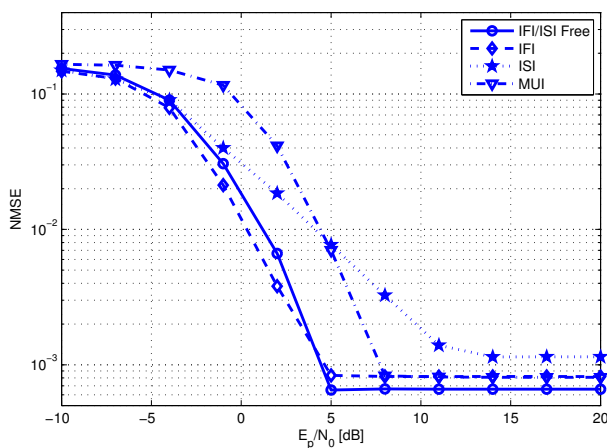


Figure 5. Performance of TCM synchronizer with  $K = 64$  symbols.

A and Test B is quite similar. This is due to fact that because of the smaller delay spread of CM1, most of channel energy resides in the same frame and out-of-frame energy affecting the next frame is not significant one. As discussed, NDA can not estimate timing offset in ISI and MUI scenarios whereas DA does estimate under

MUI but with reduced performance. However, even DA version can not succeed in the presence of ISI.

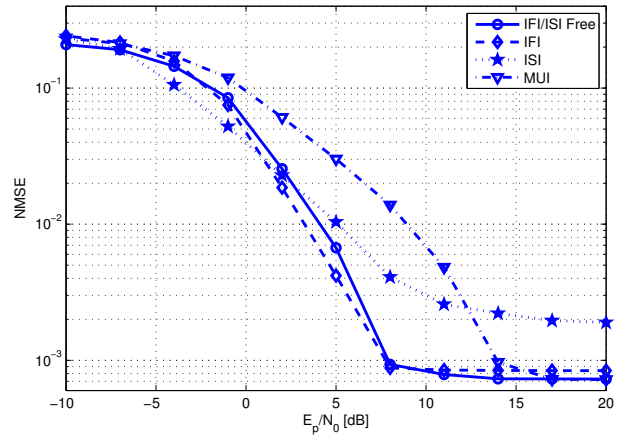


Figure 6. Performance of TED synchronizer with  $K = 64$  symbols of size  $MT_s$ .

We have assumed that information about channel delay spread was available, so both  $T_I$  and  $T_R$  are set to their optimal values in TCM and TED respectively. The curves in Figs. 5 and 6 show that both algorithms are functional in all cases, however performance is reduced significantly in MUI for TCM while in ISI for TED. One may hope this MUI performance to improve a little, if user specific polarity codes are employed in conjunction with TH codes in TCM.

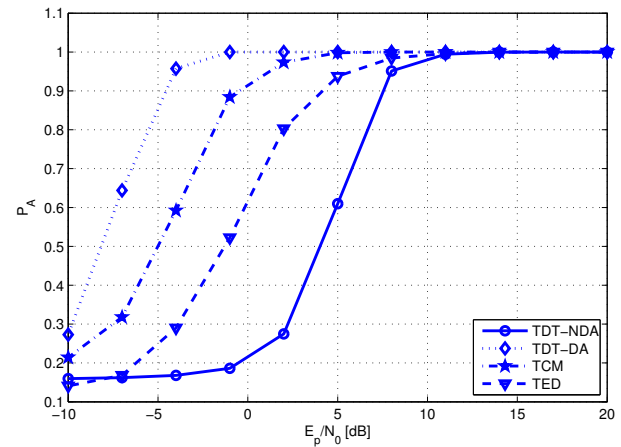


Figure 7. Comparison of TDT, TCM & TED in terms of Probability of Acquisition ( $P_A$ ) in IFI/ISI Free scenario.

Fig. 7 provides a relative comparison of three techniques under simplest case of no IFI/ISI in terms of probability of acquisition, defined as the probability that  $|\hat{\tau}_0 - \tau_0| \leq T_f$ . DA-TDT performs best among all, however it will incur rate loss due to training sequence. Among blind methods, code matching certainly outperform others. Finally, acquisition speed is determined in Fig. 8. We can see that performance of TED is highly dependent on number of symbols used, which is obvious as it is based on first-order statistics of received signal.

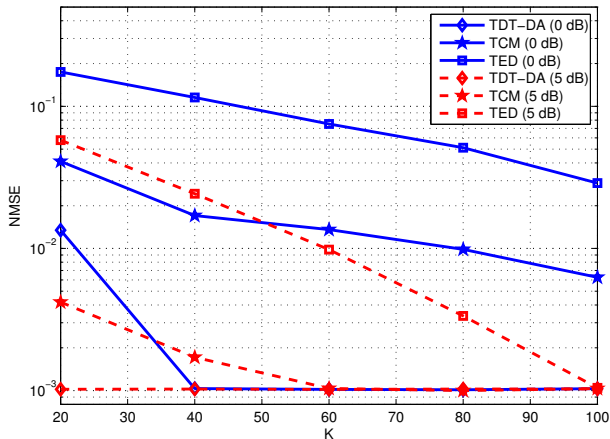


Figure 8. NMSE performance of TDT, TCM & TED in terms of number of symbols used for synchronization.

## VI. CONCLUSIONS

In this paper, we have presented an overview and comparative analysis of few blind synchronization algorithms employed in IR-UWB. These methods have formed the basis of many new schemes proposed recently for acquisition, thus understanding them will help to further dwell into the rather challenging task of synchronization. The working principle along with their limitations are presented and simulations are provided to corroborate the discussion.

## REFERENCES

- [1] "First Report and Order: In the matter of Revision of Part 15 of the Commission's Rules regarding Ultra-Wideband Transmission Systems," Federal Communications Commission, April 2002. [Online]. Available: [http://www.fcc.gov/Bureaus/Engineering\\_Technology/Orders/2002/fcc02048.pdf](http://www.fcc.gov/Bureaus/Engineering_Technology/Orders/2002/fcc02048.pdf)
- [2] M. Z. Win and R. A. Scholtz, "Impulse radio: how it works," *IEEE Commun. Lett.*, vol. 2, no. 2, pp. 36–38, Feb. 1998.
- [3] J. Balakrishnan, A. Batra, and A. Dabak, "A multi-band OFDM system for UWB communication," in *Proc. IEEE Conf. Ultra Wideband Syst. Technol.*, Nov. 2003, pp. 354–358.
- [4] L. Yang and G. B. Giannakis, "Ultra-wideband communications: An idea whose time has come," *IEEE Signal Process. Mag.*, vol. 21, no. 6, pp. 26–54, Nov. 2004.
- [5] K. Witrals, G. Leus, G. Janssen, M. Pausini, F. Troesch, T. Zasowski, and J. Romme, "Noncoherent ultra-wideband systems," *IEEE Signal. Process. Mag.*, vol. 26, no. 4, pp. 48–66, Jul. 2009.
- [6] Z. Tian and G. B. Giannakis, "BER sensitivity to mistiming in ultra-wideband impulse radios- part I: Nonrandom channels," *IEEE Trans. Signal Process.*, vol. 53, no. 4, pp. 1550–1560, April 2005.
- [7] —, "BER sensitivity to mistiming in ultra-wideband impulse radios - part II: fading channels," *IEEE Trans. Signal Process.*, vol. 53, no. 5, pp. 1897–1907, May 2005.
- [8] N. He and C. Tepedelenlioglu, "Performance analysis of non-coherent UWB receivers at different synchronization levels," *IEEE Trans. Wireless Commun.*, vol. 5, no. 6, pp. 1266–1273, June 2006.
- [9] R. J. M. Cramer, R. A. Scholtz, and M. Z. Win, "Evaluation of an ultra-wide-band propagation channel," *IEEE Trans. Antennas Propag.*, vol. 50, no. 5, pp. 561–570, 2002.
- [10] D. Cassioli, M. Z. Win, and A. F. Molisch, "The ultra-wide bandwidth indoor channel: from statistical model to simulations," *IEEE J. Sel. Areas Commun.*, vol. 20, no. 6, pp. 1247–1257, Aug. 2002.
- [11] A. F. Molisch, J. R. Foerster, and M. Pendergrass, "Channel models for ultrawideband personal area networks," *IEEE Wireless Commun.*, vol. 10, no. 6, pp. 14–21, Dec. 2003.
- [12] V. Lottici, A. D'Andrea, and U. Mengali, "Channel estimation for ultra-wideband communications," *IEEE J. Sel. Areas Commun.*, vol. 20, no. 9, pp. 1638–1645, Dec. 2002.
- [13] C. Carbonelli and U. Mengali, "Synchronization algorithms for UWB signals," *IEEE Trans. Commun.*, vol. 54, no. 2, pp. 329–338, Feb. 2006.
- [14] I. Maravic and M. Vetterli, "Low-complexity subspace methods for channel estimation and synchronization in ultra-wideband systems," in *Proc. of Intl. Workshop on Ultra-Wideband (IWUWB)*, Oulu, Finland, 2003.
- [15] Z. Tian and V. Lottici, "Low-complexity ML timing acquisition for UWB communications in dense multipath channels," *IEEE Trans. Wireless Commun.*, vol. 4, no. 6, pp. 3031–3038, Nov. 2005.
- [16] L. Yang, Z. Tian, and G. B. Giannakis, "Non-data aided timing acquisition of ultra-wideband transmissions using cyclostationarity," in *Proc. of IEEE Intl. Conf. on Acoustic, Speech and Signal Process. (ICASSP)*, Hong Kong, China, Apr. 2003, pp. 121–124.
- [17] Z. Wang and X. Yang, "Ultra wide-band communications with blind channel estimation based on first-order statistics," in *Proc. of IEEE Intl. Conf. on Acoustic, Speech and Signal Process. (ICASSP)*, Montreal, Canada, May 2004, pp. 529–532.
- [18] L. Yang and G. B. Giannakis, "Timing ultra-wideband signals with dirty templates," *IEEE Trans. Commun.*, vol. 53, no. 11, pp. 1952–1963, Nov. 2005.
- [19] S. Farahmand, X. Luo, and G. B. Giannakis, "Demodulation and tracking with dirty templates for UWB impulse radio: algorithms and performance," *IEEE Trans. Veh. Technol.*, vol. 54, no. 5, pp. 1595–1608, Sept. 2005.
- [20] M. Ouertani, H. Xu, H. Besbes, L. Yang, and A. Bouallègue, "Orthogonal bi-pulse UWB: Timing and (de)modulation," *Physical Communication*, vol. 1, no. 4, pp. 237–247, 2008.
- [21] X. Luo and G. B. Giannakis, "Blind timing and channel estimation for UWB multiuser ad hoc access," in *Asilomar Conf. Signals, Systems and Computers*, Nov. 2004, pp. vol.1, 642–646.
- [22] —, "Low-complexity blind synchronization and demodulation for (ultra-)wideband multi-user ad hoc access," *IEEE Trans. Wireless Commun.*, vol. 5, no. 7, pp. 1930–1941, July 2006.
- [23] X. Luo and G. B. Giannakis, "Cyclic-mean based synchronization and efficient demodulation for UWB ad hoc access: Generalizations and comparisons," *EURASIP J. Signal Process.*, vol. 86, no. 9, pp. 2139–2152, 2006.
- [24] X. Luo and G. B. Giannakis, "Raise your voice at a proper pace to synchronize in multiple ad hoc piconets," *IEEE Trans. Signal Process.*, vol. 55, no. 1, pp. 267–278, Jan. 2007.
- [25] R. Akbar, E. Radoi, and S. Azou, "Energy detection based blind synchronization for pulse shape modulated IR-UWB systems," in *Proc. IEEE Intl. Symp. Personal Indoor and Mobile Radio Communications (PIMRC'11)*, Sept. 2011, pp. 864–868.
- [26] Y. Ying, M. Ghogho, and A. Swami, "Code-assisted synchronization for UWB-IR systems: Algorithms and

- analysis," *IEEE Trans. Signal Process.*, vol. 56, no. 10, pp. 5169–5180, Oct. 2008.
- [27] L. Wu, V. Lottici, and Z. Tian, "Maximum likelihood multiple access timing synchronization for UWB communications," *IEEE Trans. Wireless Commun.*, vol. 7, no. 11, pp. 4497 – 4501, Nov. 2008.
- [28] B. Liu, T. Lv, and H. Gao, "Blind synchronization and demodulation for noncoherent ultra-wideband system with robustness against ISI and IFI," in *Proc. IEEE Intl. Conf. Commun. (ICC'10)*, May 2010, pp. 1 – 5.
- [29] M. Matsuo, M. Kamada, and H. Habuchi, "Design of UWB pulses based on B-splines," in *proc. IEEE Intl. Symp. on Circuits and Systems*, Japan, May 2005, pp. vol. 6, pp. 5425–5428.

**Rizwan Akbar** received his B.Sc. degree in Electrical Engineering from University of Engineering and Technology Taxila, Pakistan in 2007 and M.Sc. degree in Signals and Circuits from University of Brest, France in 2009. He is currently a PhD candidate in the department of Electronics at University of Brest. His general interests lie in wireless communications and signal processing with current focus on ultra-wideband (UWB) communications.

**Emanuel Radoi** graduated in radar systems at the Military Technical Academy of Bucharest, in 1992. In 1997 he received the M.S. degree, in electronic engineering, and in 1999 the Ph.D. degree, in signal processing, both from the University of Brest. He also received the Habilitation to Supervise Research degree in 2007 from the same university. From 1992 to 2002 he was with Military Technical Academy of Bucharest, where he developed research activities related to high resolution radar. In 2002 he joined ENSTA Bretagne, where he worked on wideband spectral and time-frequency analysis for radar imagery and high resolution sea clutter modeling.

Since 2007 he has been with the University of Brest, where he is currently Professor of Signal Processing in the Electronics department. He is also a member of the Laboratory for Science and Technologies of Information, Communication and Knowledge (CNRS, UMR 6285 Lab-STICC) and the head of the "Signal and Circuits" Research Master. His main research interests include superresolution methods, time-frequency analysis, fast digital filtering algorithms and UWB signal processing. He co-authored 7 signal processing books and more than 75 journal and conference scientific papers

**Stéphane Azou** was born in 1970. He received the M. Sc. degree in electronics, and the Ph.D. degree both from the University of Brest, Brest, France, in 1993, and 1997, respectively. He also received the HDR degree (accreditation to supervise research) from the same university in may 2007. From 1998 to 2000, he was with the Signal Processing Group at the French Naval Academy, Lanvéoc, France.

Since 2000, he has been an Associate Professor at the University of Brest. He is currently a member of the Laboratory for Science and Technologies of Information, Communication and Knowledge (CNRS, UMR 6285 Lab-STICC) and the head of "Intelligent Communication Systems" research team. His research interests include Spread-Spectrum Techniques, chaos-based communications, Communications Intelligence and signal processing for ultra-wideband (UWB) systems. He has co-authored about 40 journal and conference scientific papers.